Propagation Dynamics of Nonspreading Cosine-Gauss Water-Wave Pulses

Shenhe Fu,[1,2] Yuval Tsur,[1] Jianying Zhou,[2] Lev Shemer,[3] and Ady Arie[1,*]
[1]Department of Physical Electronics, Faculty of Engineering, Tel-Aviv University, Tel-Aviv 69978, Israel
[2]State Key Laboratory of Optoelectronic Materials and Technologies, Sun Yat-sen University, Guangzhou 510275, China
[3]School of Mechanical Engineering, Faculty of Engineering, Tel-Aviv University, Tel-Aviv 69978, Israel
(Received 15 July 2015; published 18 December 2015)

Linear gravity water waves are highly dispersive; therefore, the spreading of initially short wave trains characterizes water surface waves, and is a universal property of a dispersive medium. Only if there is sufficient nonlinearity does this envelope admit solitary solutions which do not spread and remain in fixed forms. Here, in contrast to the nonlinear localized wave packets, we present both theoretically and experimentally a new type of linearly nondispersive water wave, having a cosine-Gauss envelope, as well as its higher-order Hermite cosine-Gauss variations. We show that these waves preserve their width despite the inherent dispersion while propagating in an 18-m wave tank, accompanied by a slowly varying carrier-envelope phase. These wave packets exhibit self-healing; i.e., they are restored after bypassing an obstacle. We further demonstrate that these nondispersive waves are robust to weakly nonlinear perturbations. In the strong nonlinear regime, symmetry breaking of these waves is observed, but their cosine-Gauss shapes are still approximately preserved during propagation.

DOI: 10.1103/PhysRevLett.115.254501 PACS numbers: 47.35.Bb, 42.25.-p

The spreading of pulses in a dispersive medium is a universal property of waves. Gravity waves on the surface of deep water can be seen as an important example of a strongly dispersive wave system. As long as the wave's amplitude remains low, its evolution is adequately described by linear equations. However, for higher wave steepness, nonlinearity becomes essential. The nonlinear Schrödinger (NLS) equation [1], applicable for description of diverse nonlinear physical phenomena, is the simplest model describing evolution of narrow-banded waves in deep water. This equation attracts special interest since it admits localized solutions such as the so-called Kuznetsov-Ma breathing solitons [2,3], the Akhmediev breather [4], and the Peregrine breather [5]. Recently, there were numerous attempts to observe different types of breathers experimentally; see Refs. [6–9], among others.

In contrast to self-focusing nonlinear wave packets propagating along an experimental facility, here the question we address is whether nondispersive solutions of the linearized wave equation can be sustained along the water tank. In addition, we test the robustness of this solution in the nonlinear regime.

In optics, linearly nonspreading wave packets have been extensively investigated. Bessel beams, exact diffraction-free solutions of the Helmholtz equation in cylindrical coordinates, were introduced by Durnin *et al.* [10,11]. In Cartesian coordinates, similar solution of a nondiffracting cosine beam can also be found from this equation [12]. Recently, cosine beams were applied for realizing a nondiffracting plasmonic beam having a Gaussian envelope [13,14]. In addition to these nondiffracting beams propagating in a straight line, another example of a nondiffracting beam is the self-accelerating Airy beam, which was first suggested in the framework of quantum mechanics [15] and has been realized in optics [16]. A spatiotemporal wave packet that preserves its shape both in space and in time was also realized by combining a Bessel beam with an Airy pulse [17]. Because of their unique property, the research on nonspreading wave packets draws much attention, and many applications were demonstrated in numerous fields [18–20]. We note that nondiffracting beams have been extended to many physical systems such as surface plasmonics [13,21–23], acoustics [24,25], and electronics [26–28], described by the formally identical wave equations. Although self-accelerating Airy wave pulses and beams were recently reported in a water wave [29,30], to date, there is no report on the generation of nonaccelerating and nonspreading water wave packets.

In this Letter, we extend optical theory of nondiffracting beams to hydrodynamics and demonstrate both theoretically and experimentally a new family of surface gravity water waves, i.e., cosine-Gauss (CG) and Hermite cosine-Gauss (HCG) waves, which can resist the inherent dispersion during propagation without nonlinearity. Such an extension is possible since wave propagation dynamics in optics and hydrodynamics is analogous in many aspects [29,31,32]. Even though CG waves were previously demonstrated [12–14], to our knowledge, its higher-order versions have not been reported experimentally in any physical system. In addition to the first realization of nonspreading CG water waves, this Letter also addresses the nondispersive property of their higher-order solutions, as well as the effect of nonlinearity on these waves. Our analysis is based on the modified nonlinear Schrödinger equation [33], in which the

limitation on the spectral width in the NLS is relaxed. Following Refs. [34–36], the spatial version of the nonlinear equation in its normalized form is given by

$$\frac{\partial A}{\partial \xi}+i\frac{\partial^2 A}{\partial \tau^2}+i|A|^2A+8\varepsilon|A|^2\frac{\partial A}{\partial \tau}+2\varepsilon A^2\frac{\partial A^*}{\partial \tau}+4i\varepsilon A\frac{\partial \Phi}{\partial \tau}\bigg|_{Z=0}=0,$$
$$4\frac{\partial^2\Phi}{\partial \tau^2}+\frac{\partial^2\Phi}{\partial Z^2}=0, \qquad Z<0. \tag{1}$$

The scaled dimensionless variables are related to the physical units as $\xi=\varepsilon^2k_0x$, $\tau=\varepsilon\omega_0(x/c_g-t)$, $A=a/a_0$, $\Phi=\phi/(\omega_0a_0^2)$, and $Z=\varepsilon k_0z$. Here, x and z denote the longitudinal and vertical coordinates, where $z=0$ at undisturbed water surface, t is time, $\varepsilon=k_0a_0$ is the characteristic wave steepness, where a_0 is amplitude, and $k_0=2\pi/\lambda_0$ is the carrier wave number, with λ_0 being the wavelength. The angular frequency ω_0 satisfies the dispersion relation $\omega_0^2=gk_0$, where g is the gravity acceleration. The group velocity is $c_g=\omega_0/(2k_0)$. The velocity potential Φ is subjected to boundary conditions $\partial\Phi/\partial Z=\partial|A|^2/\partial\tau$ $(Z=0)$ and $\partial\Phi/\partial Z=0$ $(Z\to-\infty)$.

In this work, we first investigate the generation and propagation dynamics of CG pulses in the linear regime with a sufficiently low amplitude, and then investigate the robustness of these pulses under appreciable nonlinearity. Retaining linear terms only in Eq. (1) yields

$$\frac{\partial A}{\partial \xi}+i\frac{\partial^2 A}{\partial \tau^2}=0. \tag{2}$$

To look for a nonspreading cosine-Gauss solution, we assume $A(x=0,t)=\cos[\omega_0t\sin(\theta)]\exp(-t^2/t_0^2)$ [13], where θ is a half-intersecting angle of two plane waves truncated by a Gaussian envelope of finite duration t_0. Integrating Eq. (2) with this initial condition, we find

$$A(\xi,\tau)=A_0\exp(i\psi)\left\{\exp(iS\tau)\exp\left[-\frac{(\tau+2\sin(\theta)\xi/\varepsilon)^2}{T^2}\right]+\exp(-iS\tau)\exp\left[-\frac{(\tau-2\sin(\theta)\xi/\varepsilon)^2}{T^2}\right]\right\}, \tag{3}$$

where

$$A_0(\xi)=\frac{1}{2}\left(\frac{T}{\varepsilon\omega_0t_0}\right)^{-1/2},$$
$$\psi(\xi,\tau)=\frac{1}{2}\arctan\left(\frac{4\xi}{\varepsilon^2\omega_0^2t_0^2}\right)+\frac{\sin(\theta)}{\varepsilon}S\xi-\frac{4\xi}{\varepsilon^2\omega_0^2t_0^2T^2}\tau^2$$

is envelope amplitude and phase, respectively. Here, $T=\{(\varepsilon\omega_0t_0)^2+[4\xi/(\varepsilon\omega_0t_0)]^2\}^{1/2}$ and $S=\sin(\theta)/\varepsilon\{1-16\xi^2/[(\varepsilon\omega_0t_0)^4+16\xi^2]\}$. Equation (3) shows that these two finite energy waves are gradually separated in time during propagation. However, with proper parameters and small θ, $S\approx\sin(\theta)/\varepsilon$ becomes constant and $2\sin(\theta)\xi/\varepsilon\ll T$, so that these two truncated waves approximately overlap during propagation over a limited distance, giving rise to the nonspreading CG wave.

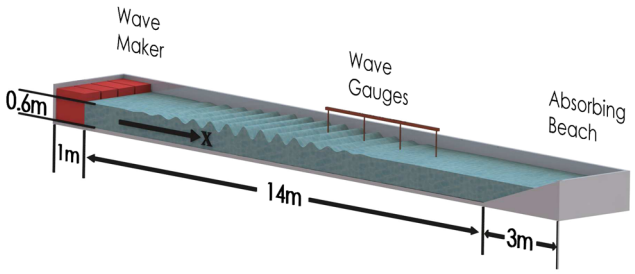

FIG. 1 (color online). Schematic illustration of the experimental setup for generating cosine-Gauss water-wave pulses.

Experiments were performed in an 18-m-long, 1.2-m-wide, and $h=0.6$-m-deep wave tank illustrated in Fig. 1. Surface CG waves were generated by means of a computer-controlled paddle-type wave maker placed at one end of the tank; see Fig. 1. An absorbing beach was placed at the other end. To avoid any influence of the beach, measurements were performed up to distances of 14 m from the wave maker. The surface elevation at any fixed location along the tank was measured by 4 wave gauges mounted on a bar parallel to propagation direction. The temporal surface elevation at the wave maker has the following form:

$$\eta(x=0,t)=a_0A(x=0,t)\cos(\omega_0t). \tag{4}$$

For the selected wavelength $\lambda_0=0.76$ m, the dimensionless depth $k_0h=4.96>\pi$ [37] satisfies the deep-water condition. Note that wave dissipation can be neglected [37] for this wavelength.

Figure 2(a) shows a straightforward way for generating a CG pulse, by launching two plane waves at an angle θ. These waves are truncated by a Gaussian envelope of finite duration t_0. The resultant field is characterized by Eq. (3). Because of the truncation, the obtained CG pulse preserves the nonspreading property over a finite distance $x_{\max}$, estimated as $x_{\max}\approx c_gt_0/\tan(\theta)$. As an example, given $t_0=9$ s and $\theta=7.5°$, we have $x_{\max}\approx37$ m with $S\approx\sin(\theta)/\varepsilon$. Typical examples of CG pulses at $x=0$ are illustrated in Figs. 2(b)–2(d) at a different θ. It is evident that the fringe distance decreases when increasing θ, as shown analytically by

$$\sigma(\theta)=\frac{0.36\pi}{\omega_0\sin(\theta)}, \tag{5}$$

where σ is the square root of the second-order moment [38]. Figure 2(e) shows this variation σ as a function of θ, in good agreement with the experiment; see calculations in Sec. (a) of Supplemental Material [39].

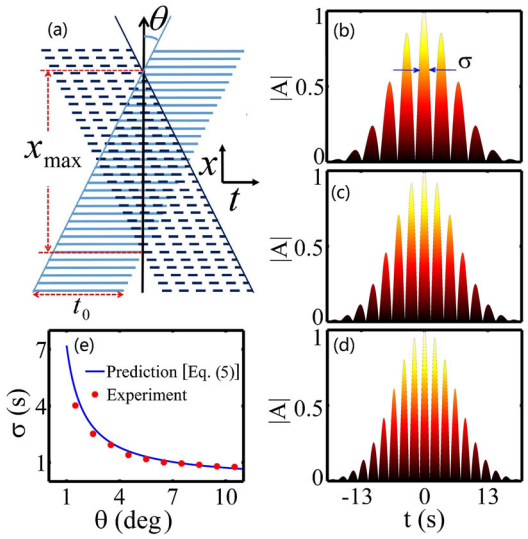

FIG. 2 (color online). (a) A schematic representing the CG pulse as a superposition of two truncated plane waves. (b)–(d) Examples for pulse profiles at $x = 0$ with $t_0 = 9$ s: (b) $\theta = 5.5°$; (c) $\theta = 7.5°$; (d) $\theta = 9.5°$. (e) Square root of second-order moment of the central lobe, as a function of θ.

Figure 3 demonstrates both experimentally and theoretically the nonspreading feature of the generated CG pulses. In experiment, we set $t_0 = 9$ s. As a result, the nonspreading region can be expected to cover the whole tank. To reduce nonlinear effects, amplitude was set to $a_0 = 6$ mm ($\varepsilon = 0.05$). The propagation dynamics of CG pulses with $\theta = 5.5°$ and $7.5°$ were investigated; see Figs. 3(a) and 3(c), respectively. Note that more narrow side lobes were observed with larger θ. Both figures present the measurements of the envelope evolution obtained by the Hilbert transform of wave elevation records. To illustrate this nonspreading property in a straight vertical line, the recorded elevations were represented in a system traveling at the group velocity c_g. As expected, these CG pulses resist the dispersion-induced broadening during propagation, preserving their symmetric CG shapes. The nondispersive property is further confirmed by the experimental and theoretical elevations at $x = 1$ and 10 m; see Figs. 3(b) and 3(d) in both cases. In comparison, a Gaussian pulse having the same initial size as in Fig. 3(a) was considered; see Figs. 3(e) and 3(f). It was observed that, due to inherent dispersion, this pulse is considerably expanding while propagating along the tank. The variation σ of CG and Gaussian pulses along the tank was also measured; see Sec. (a) of Supplemental Material [39].

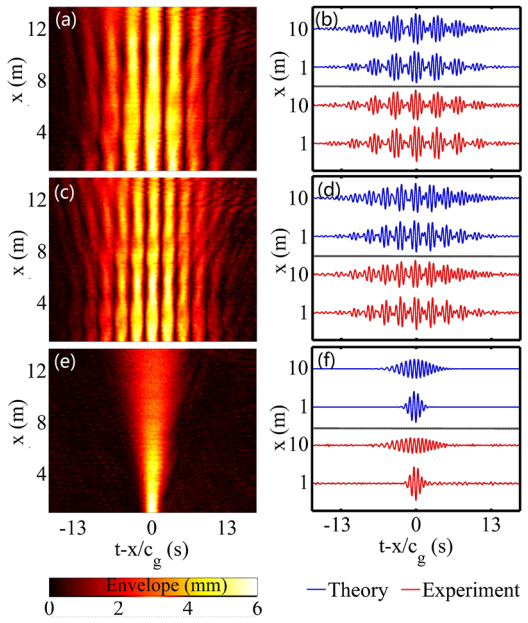

FIG. 3 (color online). Propagation dynamics of CG pulses along the tank with $a_0 = 6$ mm, $t_0 = 9$ s, and $\theta = 5.5°$ (a),(b) and $\theta = 7.5°$ (c),(d). (a),(c) Experimental measurements of pulse envelopes obtained by Hilbert transform, while (b),(d) show temporal elevations at two locations. (e),(f) Gaussian pulse evolution. The Gaussian pulse initial size is the same as (a).

It was reported that by extracting the local maximum and minimum values of the elevation the envelope phase can be demodulated [29]. Here, we presented a different method based on Hilbert transform to directly measure the induced envelope phase variation. To demonstrate this, we recorded wave elevation η_j at two specific locations x_j ($j = 1, 2$), with η_1 being the reference. The induced envelope phase ψ can be determined by their phase difference; see detailed calculations in Sec. (d) of Supplemental Material [39]. Using this method, we measured the evolutions of envelope phase ψ illustrated in Fig. 4 with two different θ, within an accuracy of $\cos(\psi) \pm 0.2$. It demonstrates in both cases that for a fixed location ψ changes very slowly with time, accompanied by a phase offset that has a nonlinear dependence on the location [see Eq. (3)]. We attribute this phenomenon to the nonspreading feature of CG pulses,

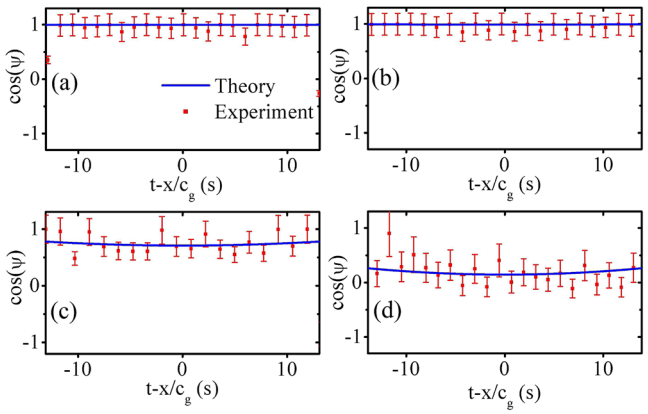

FIG. 4 (color online). The measured carrier-envelope phase ψ of CG pulses with $a_0 = 6$ mm, $t_0 = 9$ s, and $\theta = 5.5°$ (a),(c) and $\theta = 7.5°$ (b),(d). Measurements were performed at (a),(b) $x = 1$ m and (c),(d) $x = 10$ m. Red symbols and blue curves correspond to experiment and theory [based on Eq. (3)].

generated by interfering two Gaussian waves at a small intersection angle. A slight difference between the experiment and theory resulted from small deviation of the elevation generated by the wave maker, as compared with the theory.

We examined the self-healing property of the cosine-Gauss pulse experimentally and numerically; see Sec. (b) in Ref. [39]. We found that these wave packets can be restored after bypassing an obstacle. Interestingly, those cosine-Gauss pulses could also be realized dynamically by utilizing two propagating Gaussian pulses; see Sec. (c) in Ref. [39] for more detail.

We further extended the concept of CG pulses to their higher-order forms with Hermite CG envelopes. In the experiment, the pattern produced at $x = 0$ is replaced by the HCG function

$$A(x=0,t) = H_m\left(\frac{\sqrt{2}t}{t_0}\right)\cos[\omega_0 t\sin(\theta)]\exp\left(-\frac{t^2}{t_0^2}\right), \quad (6)$$

where H_m $(m = 1, 2)$ represents the Hermite polynomial of order m. In this case, $A(x = 0, t)$ is normalized to unity, so that a_0 is the maximum amplitude of the envelope. Experimental and numerical results for the evolution dynamics of these HCG pulses are presented in Fig. 5. Clearly, these higher-order pulses also exhibit the non-spreading property and preserve their symmetric HCG shapes, which was observed from both the envelope evolutions [see Figs. 5(a) and 5(c)] and elevations [see Figs. 5(b) and 5(d)]. Owing to the limited value of t_0, fewer side lobes were generated. As a consequence, these side lobes as well as the central lobe in Fig. 5(c) become more dispersive during propagation, but the main lobes, see the arrows in Figs. 5(a) and 5(c), are nearly nondispersive, keeping their width unchanged. Theoretically, the width of the main lobes of CG and HCG pulses should be the same, described by Eq. (5). We confirm this assertion by measuring their square root σ; see calculations in Sec. (a) in Ref. [39].

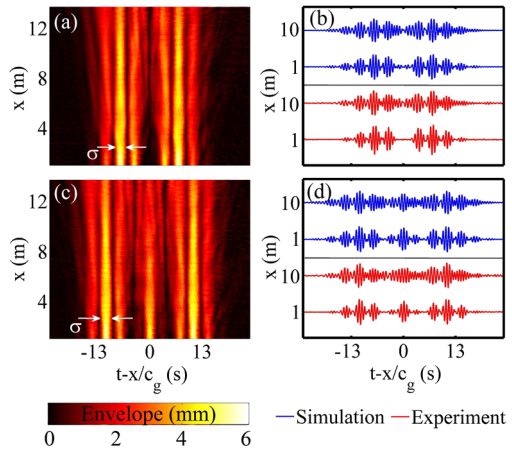

FIG. 5 (color online). Propagation dynamics of HCG pulses with $t_0 = 9$ s, $\theta = 5.5°$, and $a_0 = 6$ mm. (a),(b) $m = 1$ and (c), (d) $m = 2$. (a),(c) The experimental measurements of pulse envelopes, while (b),(d) show the corresponding elevations.

Finally, we examined the robustness of CG water waves to nonlinear perturbations. To date, the research on cosine-Gauss waves was limited only to the linear approximation [13,14] and their propagation dynamics in a nonlinear dispersive medium was never explored. Our nonlinear study of CG pulses is based on the modified NLS equation, i.e., Eq. (1) for the HG_0 and HG_1 envelopes. Whereas the HCG_0 wave maintains maximum intensity at the center of the pulse, the HCG_1 pulse has zero intensity at the center, but preserves the two strong nearby peaks at the leading and trailing edges of the pulse; see Fig. 6. For a weakly nonlinear amplitude of $a_0 = 16$ mm $(\varepsilon = 0.13)$, see Figs. 6(a) and 6(e), it was found that the invariant propagation of such HCG pulses was still observed despite weak nonlinearity. Moreover, these HCG pulses become more stable: the lower amplitude side lobes become less dispersive, as compared with the linear regime [see Figs. 3(c) and 5(a)]. The pulse dispersion from the side lobes was compensated by the weak focusing nonlinearity. Surprisingly, for a high amplitude $a_0 = 26$ mm $(\varepsilon = 0.22)$, see Figs. 6(c) and 6(g), despite the slight symmetry breaking of its temporal distribution, HCG pulses still maintain their general shapes while propagating along the tank. This behavior is very different from the self-accelerating Airy wave, in which for high nonlinearity the wave packet becomes unstable as it breaks and solitons emerge at directions that are different from the original wave trajectory [29,40,41]. We note that a slight asymmetric distribution of HCG pulses arises from the contribution of two quadratic nonlinear terms of Eq. (1). We compared experimental results with simulations, showing a good correspondence; see Figs. 6(b) and 6(f) and Figs. 6(d) and 6(h), respectively.

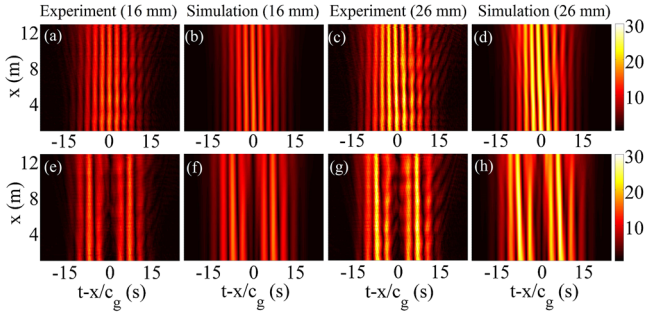

FIG. 6 (color online). Nonlinear propagation dynamics of HCG_0 (a)–(d) and HCG_1 (e)–(h) pulses for two typical amplitudes (see the top), with parameters (a)–(d) $t_0 = 9$ s, $\theta = 7.5°$ and (e)–(h) $t_0 = 9$ s, $\theta = 5.5°$. Both the experiments and simulations [based on Eq. (1)] show pulse envelope evolutions along the tank. The color bar units are millimeters.

In conclusion, we extended the concept of optical nondiffracting wave packets to hydrodynamics and generated a new type of linearly nondispersive water waves. In addition to the water-wave Airy pulses [29], this is another kind of linearly nonspreading wave packets, preserving their shapes along a straight line. Their nonspreading and self-healing [39] properties, as well as carrier-envelope phase evolution, were studied in detail. Furthermore, we studied the stability of CG pulses to the nonlinear perturbations. We found that HCG waves are very robust to weak nonlinear perturbations, and exhibit slight symmetry breaking in the strong nonlinear regime. This property is not limited to our experimental facility. In a general case, our numerical simulation indicates that these waves could approximately preserve their general shapes across the entire nonspreading region even with stronger nonlinear perturbations, characterized by a scaled distance of $\xi = 9.9$. Owing to the similar wave nature, we anticipate that these results will motivate intriguing studies of such nonspreading wave packets in other physical systems such as electronics [26], acoustics [24], and plasma waves [13,14].

This work was supported by DIP, the German-Israeli Project cooperation, the Israel Science Foundation (Grant No. 1310/13), the National Basic Research Program (Grant No. 2012CB921904), the U.S.-Israel Binational Science Foundation (Grant No. 2010219), and the Overseas Study Program of China Scholarship Council.

*ady@eng.tau.ac.il

[1] V. E. Zakharov, J. Appl. Mech. Tech. Phys. **9**, 190 (1968).
[2] E. A. Kuznetsov, Dokl. Akad. Nauk SSSR **236**, 575 (1977) [Sov. Phys. Dokl **22**, 507 (1977)].
[3] Y. C. Ma, Stud. Appl. Math. **60**, 43 (1979).
[4] N. N. Akhmediev, V. M. Eleonskii, and N. E. Kulagin, Theor. Math. Phys. **72**, 809 (1987).
[5] D. H. Peregrine, J. Aust. Math. Soc. Series B, Appl. Math. **25**, 16 (1983).
[6] A. Chabchoub, N. P. Hoffmann, and N. Akhmediev, Phys. Rev. Lett. **106**, 204502 (2011).
[7] A. Chabchoub and M. Fink, Phys. Rev. Lett. **112**, 124101 (2014).
[8] L. Shemer and L. Alperovich, Phys. Fluids **25**, 051701 (2013).
[9] L. Shemer, Proc. Estonian Acad. Sci. **64**, 356 (2015).
[10] J. Durnin, J. Opt. Soc. Am. A **4**, 651 (1987).
[11] J. Durnin, J. J. Miceli, Jr., and J. H. Eberly, Phys. Rev. Lett. **58**, 1499 (1987).
[12] J. C. G. Vega and M. A. Bandres, J. Opt. Soc. Am. A **22**, 289 (2005).
[13] J. Lin, J. Dellinger, P. Genevet, B. Cluzel, F. de Fornel, and F. Capasso, Phys. Rev. Lett. **109**, 093904 (2012).
[14] I. Epstein, Y. Lilach, and A. Arie, J. Opt. Soc. Am. B **31**, 1642 (2014).
[15] M. V. Berry and N. L. Balazs, Am. J. Phys. **47**, 264 (1979).
[16] G. A. Siviloglou, J. Broky, A. Dogariu, and D. N. Christodoulides, Phys. Rev. Lett. **99**, 213901 (2007).
[17] A. Chong, W. H. Renninger, D. N. Christodoulides, and F. W. Wise, Nat. Photonics **4**, 103 (2010).
[18] V. G. Chávez, D. McGloin, H. Melville, W. Sibbett, and K. Dholakia, Nature (London) **419**, 145 (2002).
[19] J. Baumgartl, M. Mazilu, and K. Dholakia, Nat. Photonics **2**, 675 (2008).
[20] P. Polynkin, M. Kolesik, J. V. Moloney, G. A. Siviloglou, and D. N. Christodoulides, Science **324**, 229 (2009).
[21] A. Minovich, A. E. Klein, N. Janunts, T. Pertsch, D. N. Neshev, and Y. S. Kivshar, Phys. Rev. Lett. **107**, 116802 (2011).
[22] P. Zhang, S. Wang, Y. Liu, X. Yin, C. Lu, Z. Chen, and X. Zhang, Opt. Lett. **36**, 3191 (2011).
[23] L. Li, T. Li, S. M. Wang, C. Zhang, and S. N. Zhu, Phys. Rev. Lett. **107**, 126804 (2011).
[24] P. Zhang, T. Li, J. Zhu, X. Zhu, S. Yang, Y. Wang, X. Yin, and X. Zhang, Nat. Commun. **5**, 4316 (2014).
[25] Z. Lin, X. Guo, J. Tu, Q. Ma, J. Wu, and D. Zhang, J. Appl. Phys. **117**, 104503 (2015).
[26] N. V. Bloch, Y. Lereah, Y. Lilach, A. Gover, and A. Arie, Nature (London) **494**, 331 (2013).
[27] R. Shiloh, Y. Tsur, R. Remez, Y. Lereah, B. A. Malomed, V. Shvedov, C. Hnatovsky, W. Krolikowski, and A. Arie, Phys. Rev. Lett. **114**, 096102 (2015).
[28] V. Grillo, E. Karimi, G. C. Gazzadi, S. Frabboni, M. R. Dennis, and R. W. Boyd, Phys. Rev. X **4**, 011013 (2014).
[29] S. Fu, Y. Tsur, J. Zhou, L. Shemer, and A. Arie, Phys. Rev. Lett. **115**, 034501 (2015).
[30] U. Bar-Ziv, A. Postan, and M. Segev, Phys. Rev. B **92**, 100301 (2015).
[31] J. M. Dudley, F. Dias, M. Erkintalo, and G. Genty, Nat. Photonics **8**, 755 (2014).
[32] A. Chabchoub, B. Kibler, C. Finot, G. Millot, M. Onorato, J. M. Dudley, and A. V. Babanin, Ann. Phys. (Amsterdam) **361**, 490 (2015).
[33] K. B. Dysthe, Proc. R. Soc. A **369**, 105 (1979).
[34] E. Lo and C. C. Mei, J. Fluid Mech. **150**, 395 (1985).
[35] E. Kit and L. Shemer, J. Fluid Mech. **450**, 201 (2002).
[36] L. Shemer and B. Dorfman, Nonlinear Processes Geophys. **15**, 931 (2008).
[37] L. Shemer, K. Goulitski, and E. Kit, Eur. J. Mech. B, Fluids **26**, 193 (2007).
[38] H. Weber, Opt. Quantum Electron. **24**, S1027 (1992).
[39] See Supplemental Material at http://link.aps.org/supplemental/10.1103/PhysRevLett.115.254501 for (a) second-order moment of cosine-Gauss pulses, (b) self-healing of cosine-Gauss pulses, (c) generation of cosine-Gauss pulses by two traveling Gaussian waves, and (d) phase measurement by Hilbert transform.
[40] Y. Fattal, A. Rudnick, and D. M. Marom, Opt. Express **19**, 17298 (2011).
[41] I. M. Allayarov and E. N. Tsoy, Phys. Rev. A **90**, 023852 (2014).